

Joint Design for Electric Fleet Operator and Charging Service Provider: Understanding the Non-Cooperative Nature

Yiqi Zhao^{ID}, Teng Zeng^{ID}, Zaid Allybokus^{ID}, Ye Guo^{ID}, *Senior Member, IEEE*,
and Scott Moura^{ID}, *Member, IEEE*

Abstract—This work proposes a new modeling framework for jointly optimizing the charging network design and the logistic mobility planning for an electric vehicle fleet. Existing literature commonly assumes the existence of a single entity – the social planner, as a powerful decision maker who manages all resources. However, this is often not the case in practice. Instead of making this assumption, we specifically examine the innate non-cooperative nature of two different entities involved in the planning problem. Namely, they are the charging service provider (CSP) and the fleet operator (FO). To address the strategic interaction between entities, a bi-level mixed integer program is formulated, with the CSP/FO's problem expressed in the upper/lower levels respectively, in a joint decision making process. These decisions involve the CSP's infrastructure siting, sizing, substation capacity upgrades, the FO's fleet composition, vehicle routing, charging, and delivery assignment. To solve the problem, an iterative fashion is adopted to solve and reach optimality. We conduct detailed numerical studies on a synthesized small network and the simulation results reveal the unique aspects of this two-entity framework. This modeling perspective can be generalized to other system design problems with two interacting agents planning and operating resources across networks.

Index Terms—Electric trucks, heterogeneous fleet sizing, charging infrastructure planning, stackelberg game.

I. INTRODUCTION

DECARBONIZATION of the transportation sector is an important step towards alleviating climate change. In the U.S., about 28% of the total greenhouse gas emissions is contributed by transportation [1]. According to the California Air Resources Board (CARB), commercial trucks are responsible for 80% of the diesel soot emitted, leading the largest source of air pollution from vehicles [2]. Hence, a significant step

to cut emissions is electric commercial vehicles, specifically E-trucks, as part of a sustainable supply chain. As a result, CARB has voted to rule out the sales of any fossil fuel trucks by 2045 and to force truck makers to begin the transition in 2024 [2].

Along with enforcing policy orders, many logistic and delivery companies (we refer to as fleet operators, FOs) and Charging Service Providers (CSPs) are committed to transportation electrification. To realize profit maximization, it is more important to have effective communications between these two entities. The CSPs, with knowledge of spatial-temporal charging demands, could strategically construct their charging network to accommodate the needs; whereas the FOs, whose electrified trucks are constrained by driving range, would consider charging en-route but with minimal detours.

A. Literature Review

In this section, we are going to review a body of literature that we have identified as not only relevant but also crucial to understand our problem. On one hand, to consider commercial E-trucks routing, a portfolio of attributes can be considered, including *homogeneous/heterogeneous fleet, range, partial/fully charging time, delivery time windows, etc.* On the other hand, to consider charging infrastructure planning, another set of attributes are considered, such as *the station locations, power constraints, etc.* The two entities, FO and CSP, are entangled through charging events and an extensive body of literature ([3], [4], [5], [6], [7], [8], [9], [10], [11]) has accounted for this interactions. In the field of Operation Research and Electrical Engineering, this is called the electric location routing problem (E-LRP), an extension to pure electric vehicle routing problem (E-VRP). For the classical vehicle/location routing problems, we refer interested readers to these two survey papers [12], [13].

In the aforementioned literature, each work varies focus slightly and considers a subset of the above entity-specific attributes. Yang and Sun [3] were the first to investigate the E-LRP, where the location of battery swapping stations (BSS) was jointly optimized together with the routing of a homogeneous E-trucks fleet. The computational results of the work were later improved by Hof, Schneider and Goeke [4]. M. Schiffer et al. conducted a series of research on E-LRPs. Each publication in this series has a different focus. For example, [5] incorporated real-world data to address the competitiveness between E-trucks and ICEVs, [6], [7] considered

Manuscript received 22 March 2021; revised 4 November 2021 and 19 June 2022; accepted 13 October 2022. Date of publication 28 October 2022; date of current version 26 January 2023. This work was supported in part by TotalEnergies. The Associate Editor for this article was A. Hajbabaie. (Yiqi Zhao and Teng Zeng contributed equally to this work.) (Corresponding author: Teng Zeng.)

Yiqi Zhao and Ye Guo are with the Smart Grid and Renewable Energy Laboratory, Tsinghua-Berkeley Shenzhen Institute, Tsinghua University, Shenzhen 518055, China.

Teng Zeng is with the Department of Civil and Environmental Engineering, University of California at Berkeley, Berkeley, CA 94720 USA (e-mail: tengzeng@berkeley.edu).

Zaid Allybokus is with TotalEnergies OneTech, 92078 Paris La Défense Cedex, France.

Scott Moura is with the Smart Grid and Renewable Energy Laboratory, Tsinghua-Berkeley Shenzhen Institute, Tsinghua University, Shenzhen 518055, China, and also with the Department of Civil and Environmental Engineering, University of California at Berkeley, Berkeley, CA 94720 USA.

Digital Object Identifier 10.1109/TITS.2022.3215926

deployment of multiple types of facilities (replenishment, recharging, and combined type facilities), [8] addressed uncertainty using robust optimization, [9] used different planning objectives. Authors in [10] further considered multiple types of charging facilities in E-LRP with time windows (E-LRPTW). Paper [11], on the other hand, investigated the effects of heterogeneous fleets on a similar E-VRPTW setting with a full recharge scheme. These works inevitably assume the existence of a powerful social planner, who is capable of coordinating all the tasks. However, this is often not possible in practice. Instead, the FO and the CSP are more likely to be separate organizations with misaligned incentives, leading to non-cooperative behavior. Such interactions exist in other domains, power system transmission expansion [14], distribution system and demand response [15], food products supply chain [16], forestry and biofuel supply chain [17]. In the EV domain, a recently published paper [18] discussed a Stackelberg game setting for the private electric vehicles, in which charging facility locations, capacities and prices were the main focuses. However, the routing decisions for delivery, the charging schedule, the time windows are outside of their scope. Reference [6] included both the charging station siting and fleet sizing decisions, but a single planner was assumed. In this work, we specifically capture these dynamics and model it as a leader-follower Stackelberg Game, which to the authors' best knowledge, has never been studied.

Furthermore, the modeling approaches in the above works closely resemble each other and are the natural stems from the classic traveling salesman problem (TSP). The abstracted network is often called the customer-node based network, where customer nodes are the graph representatives and constrained to be visited once and exactly once. Additional features like range limits and charging speed for E-trucks are easily incorporated via supplemental constraints.

On the other hand, while the customer-node based network is classic and easy to adopt, the shortfall is prominent - lack of flexibility in tracking temporal events, such as charging. Since every node is associated with one specific set of entry and exit times for one vehicle, the temporal sense of simultaneous visits or queuing at a charging station node is dismissed. Adding trackers, e.g. indicator functions, is inevitable to address this issue. However, this makes the problem highly nonlinear and hence the solution quality cannot be guaranteed. Alternatively, references [19], [20] adopted the idea of layered graphs and proposed state-space-time/resource-space-time expanded networks to embed discretized resource values (energy consumption, time, etc.) when defining nodes. In this case, resource constraints are directly encoded in the expanded network model and time-dependent consumption patterns can be characterized. However, such modeling flexibility comes at a cost of significantly increased network size, and subsequently the problem scale. To plan a charging network, authors from [21] took a macroscopic point of view with traffic flow and designed another way to expand the transportation network. In this network, all reachable nodes are extended with hyper-arcs to model EVs' feasible routes. Then, a joint fleet sizing and charging system planning method for autonomous electric vehicles was proposed. However, the core, which is

TABLE I
OVERVIEW OF CONSIDERED ASPECTS IN EXISTING LITERATURE

Ref.	View-point	Fleet Design	CS* Design	Charging Option	Logistic Cons.	TW*	CS Cons.
[11]	FO*	heter	×	Fully	✓	✓	×
[22]	FO	×	×	Partial	×	✓	×
[23]	FO	×	×	Fully	×	✓	✓
[8]	SP*	homo	site	Partial	✓	✓	×
[3]	SP	×	site	Fully	✓	×	×
[20]	SP	×	site	Partial	✓	✓	×
[21]	SP	homo	size	Fully	×	×	✓
Our	Multi-players	heter	site +size	Partial	✓	✓	✓

* CS: charging station; TW: time window at customer points; FO: fleet operator; SP: social planner.

the extended network, requires full recharge and predefined homogeneous battery capacities. Recently, the authors of [22] introduced a novel mixed integer linear programming model for the E-VRP with load-dependent charging patterns. The proposed formulation allows multiple visits of charging stations without expanding the network into higher dimensions, thus helping to reduce the problem scale. Although this approach neatly relaxes the aforementioned restriction, it cannot be directly applied to a setting where locations of charging facilities are unknown. To conclude, though charging station location planning for E-trucks has been studied, incorporating station size and capacity upgrade remains as gap in this field of research.

We have reviewed a series of literature and identified the remaining gaps in the community. In Table I, we summarize the aspects covered by some representative works and compare with ours.

B. Contributions

This paper proposes a novel framework to jointly consider the charging infrastructure deployment and E-truck fleet design, as well as routing strategies. In this paper, we consider two players (the CSP and FO) who jointly optimize their decisions, under their individual objectives, and explore if the solution leads to a sense of non-cooperation. Note that in practice, stochastic conditions are indeed a big challenge, yet this manuscript is not focused on addressing that. It focuses on the two specific entities with misaligned objectives. This issue is poorly understood. Comparing to existing literature, the major innovations of this paper are:

- 1) Instead of assuming the existence of a powerful single entity who owns both the fleet and the charging network, a two-party model with the charging service provider and fleet operator is adopted. They have their own objectives and their interactions are captured via a Stackelberg game, whose results are closely analyzed. This modeling perspective, to the authors' best knowledge, has never been studied for the vehicle/location routing problem before. The necessity of such modeling perspective is revealed.
- 2) We propose an innovative partial time expanded network (PTEN) model on top of the customer-node based network [3], [4], [5], [6], [7], [8], [9], [10], [11], [24]. This network only expands at candidate charging station

nodes to capture both the time domain index and the charger index. This enables us to track the simultaneous charging activities of E-trucks at each location. Therefore, we may incorporate not only the charging station location but also the size decisions. Based on this, the upgrade cost of transformers is also incorporated in the CSP cost calculation, which is actually an important factor in real-world operation but has been neglected in past research. The PTEN also keeps the overall model in the domain of mixed integer linear program, which is more tractable than a mixed integer non-linear program.

In order to solve this complex problem, the framework is broken down to be solved in an iterative fashion. An outer loop adopts the idea from [25] to capture the dynamics of the Stackelberg game while ensuring convergence. Within each iteration, three subproblems are solved for CSP, FO, and a feasibility check accordingly. Each subproblem can be solved by either an off-the-shelf solver or any customized algorithm. We emphasize our contributions to the modeling perspective, rather than a particular solution algorithm.

The remainder of this paper is organized as follows: Section II gives formal problem definition and the proposed partial time expanded network modeling method. Based on the system model, Section III presents the detailed mathematical formulations of the planning problem. The solution algorithm for the formulated model is then described in Section IV. Case studies are presented in Section V followed by the conclusions and limitations in Section VI.

II. PROBLEM DEFINITION AND SYSTEM MODEL

The overall goal of this paper is to optimally design the E-truck fleet composition and associated charging station network. Specifically, a charging service provider decides where to locate new CSs among candidate locations. Additionally, the number of charging ports and substation capacity upgrades (size configurations) are optimized. A fleet operator designs the portfolio of fleet vehicle types, and the optimal routing and charging strategies to deliver customer demands within given time windows while avoiding battery depletion. In this section, we define the problem and present the intuitive illustration to our proposed model.

A. Problem Description

The problem is defined on a directed graph $\mathcal{G} = \{\mathcal{E}, \mathcal{V}\}$, where \mathcal{E} is the set of all edges¹ and \mathcal{V} is the collection of all nodes. Specifically, nodes in \mathcal{V} are categorized into three different types: a depot node D_0 , customer nodes $\{C_1, C_2, \dots, C_n\}$ in set \mathcal{C} , and candidate charging station (CS) nodes $\{F_1, F_2, \dots, F_m\}$ in set \mathcal{F} . Successive visits of nodes are represented with chosen edges. This is the aforementioned *customer-node based network*. We assume the following common rules:²

- 1) All customer nodes are visited once and only once by one vehicle during one duty cycle.

¹We will use edge, link, and arc interchangeably.

²Background on the vehicle routing problem and its common formulations can be found in [3], [4], [5], [6], [7], [8], [9], [10], [11], and [24].

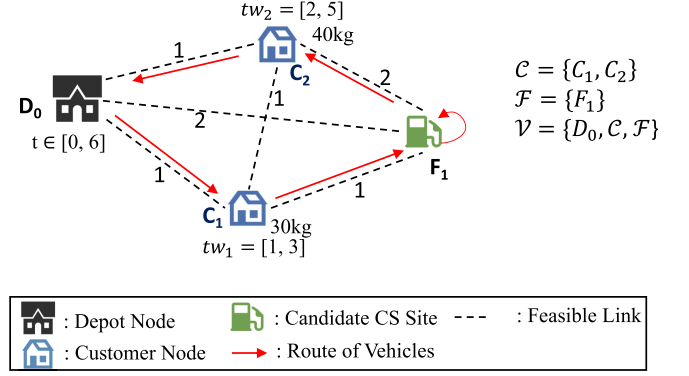


Fig. 1. Illustrative network.

- 2) All E-trucks depart from the depot D_0 and return to the same depot after completing the assigned logistic tasks.
- 3) Customer demands are represented in the aggregate sense with real values and without specifications, e.g. weight, size, or shape.

An illustrative network and toy example is given in Fig.1. One depot D_0 , two customer nodes C_1 and C_2 , and one charging node F_1 , dashed lines indicate feasible links. Assume there is an E-truck with a driving range of 4 units of length. One possible route is colored in red with arrow directing its trajectory: the E-truck will first make a stop at C_1 due to given time window $[1,3]$, then recharge at F_1 and go to C_2 , whose latest required arrival time is 5. Upon task completion, the E-truck will make a return to D_0 . Alternatively, the feasible routing plan can be chosen as $D_0 - C_1 - D_0$ and $D_0 - C_2 - D_0$. Hence, recharging is not required, but two E-trucks are needed to fulfill the task.

In this model, every time index is inherently associated with the node. We loose information to concurrent charging sessions when multiple E-trucks are traversing on the graph. Hence, the model is unable to consider configurations of the charging infrastructure, i.e. the number of ports and transformer upgrades. A work-around is introducing indicator functions to determine specific charging periods; or full state-space-time layered graph is used (Section I-A). Both approaches either impose nonlinearities or severe scaling issues (number of nodes and links explodes). In the next subsection, we propose a different graph expansion approach to capture the time information neatly.

B. Proposed Model: Partial Time Expanded Network Model

We propose to encode the time expansion solely on the charging station nodes, avoiding other unnecessarily added nodes. Namely, this is a partial time expansion. Each original candidate CS node $F_i \in \mathcal{F}$ is expanded across time and charging ports. A two-dimensional time-port graph (Fig.2) is introduced to represent a candidate CS node. Altogether, $|T_i| \cdot |s_i|$ dummy nodes³ are introduced to represent node F_i , where $|T_i|$ is the time horizon (i.e. the number of feasible visiting time slots at F_i) and $|s_i|$ is the CS size (i.e. the number of charging ports). Each of these nodes, as shown in Fig.2,

³We will use dummy nodes, dummies, and virtual nodes interchangeably.

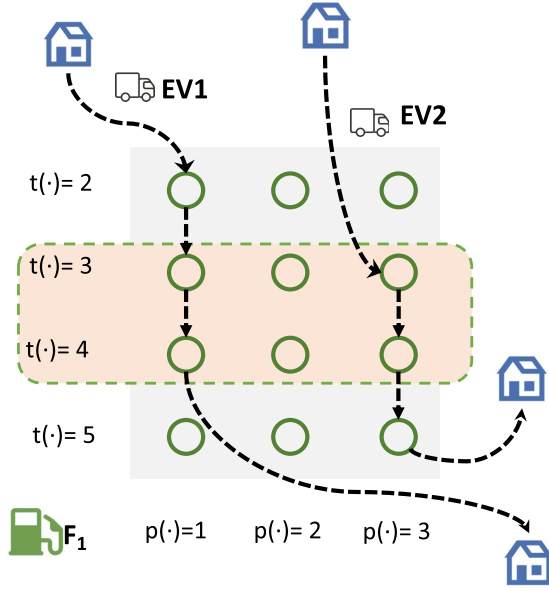


Fig. 2. An example for a partial time expanded charging station.

encodes two index trackers: the time availability index $t(\cdot)$ and the charging port index $p(\cdot)$. We denote a set \mathcal{M}_i to represent these expanded nodes.

We have defined nodes and now will construct feasible links between nodes within this set \mathcal{M}_i . A link from node j to node m , $\{j, m \in \mathcal{M}_i\}$, is created if $t(m) - t(j) = \Delta t$ and $p(m) = p(j)$, indicating an E-truck charges at port $p(j)$ for one time step (Δt) starting at $t(j)$. We denote the set of all internal links at station node F_i as \mathcal{A}_i . A subset of time specific links is defined as $\mathcal{A}_i(t) = \{(j, m) \in \mathcal{A}_i \mid t(j) = t, t(m) = t + \Delta t\}$. The original links connecting between customer nodes and the station nodes are reconnected accordingly. With this expansion, real time charging power at station F_i can be easily computed by counting the number of traversed links in $\mathcal{A}_i(t)$. Take the case in Fig. 2 as an example, the connection represents that E-truck 1 charges during period $[2, 4]$ and E-truck 2 charges during $[3, 5]$. Hence, at least two chargers are needed as both E-trucks are present during time $[3, 4]$ (box color coded).

A copy of the depot node is also created as the sink node D'_0 (due to assumption 1, this is a common practice). A corresponding partial time expanded network is presented in Fig.3. The charging activity at F_1 is then modeled by the link $(F_1 - 1 - 2, F_1 - 1 - 3)$.

We will denote the expanded network as $\mathcal{G}^{PTE} = \{\mathcal{E}^{PTE}, \mathcal{V}^{PTE}\}$. Formal notations are summarized in Table II, but relevant sets are also given in Fig.1 and Fig.3. We present the nomenclature in Table III and are now ready to formally introduce the planning problem formulation in the following section.

III. MATHEMATICAL FORMULATION OF THE PROBLEM AS BI-LEVEL PROGRAMMING

As mentioned in previous sections, this study aims to capture the interactive dynamics between the charging service provider and the fleet operator. We do not assume cooperation

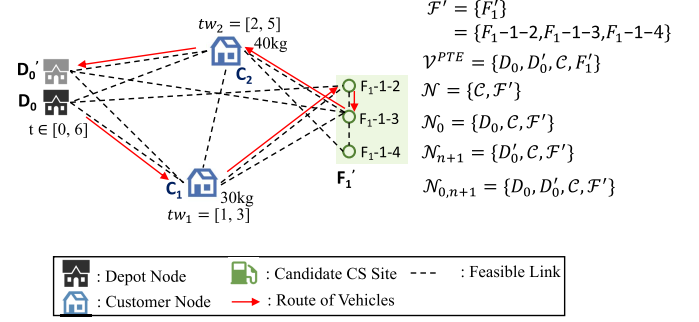


Fig. 3. Expanded illustrative network. Here, the notation $F_1 - x - y$ represents the x^{th} charger and the corresponding time slot y .

TABLE II
NODES AND LINKS BEFORE AND AFTER NETWORK EXPANSION

Network	Nodes
\mathcal{G}	$\mathcal{V} = \{D_0, C, F\}$
\mathcal{G}^{PTE}	$\mathcal{V}^{PTE} = \mathcal{V} \cup D'_0 \cup \{F' = \{\mathcal{M}_i \mid i \in \mathcal{F}\}\} \setminus \mathcal{F}$
	Arcs
\mathcal{G}	$\mathcal{E} = \{(i, j) \mid i, j \in \mathcal{V}, i \neq j\}$
\mathcal{G}^{PTE}	$\mathcal{E}^{PTE} = \{(i, j) \mid i, j \in \mathcal{V}^{PTE}, i \neq j\} \setminus \{(i, j) \mid i, j \in \mathcal{F}'_k, t(i) - t(j) \neq \Delta t\}$

between these two players and hence competition between the two entities is inevitable. Today, many transportation logistic companies are considering fleet electrification to reduce total cost of ownership, reduce greenhouse gas emissions, and satisfy upcoming regulations [26], [27], [28]. However, optimally designing the vehicle fleet, routing, and charging strategies remains as open questions. Fleet operators, as we observed, often seek consultation from charging service providers in practice. This naturally leads to a leader-follower setting, in which the charging service provider is the leader.⁴ We assume leader is the CSP in this work and has complete information of the follower. Leader-follower games are also known as Stackelberg games [29].

The decision variables and notation for the problem are summarized in Table III. Next, we detail the model for each player as well as for the complete problem.

A. CSP's Problem: Charging Network Design and Operation

The leader CSP aims to minimize its overall costs by optimally placing and sizing the new charging stations. The binary variable y_i is used to indicate the construction decision at the specific site F_i , and the integer variable s_i represents the number of chargers to be installed at F_i .

The overall cost g^L constitutes two parts. The first part is the capital expenditure (CAPEX), namely the costs for installing ports and for upgrading the local transformer if necessary. The second part is the operational profit introduced by providing charging service to E-trucks with the predetermined service fee c_i^e (\$/kWh). Mathematically, g^L is expressed as

$$g^L(\mathbf{y}, \mathbf{s}, \Delta \mathbf{P}) = \sum_{i \in \mathcal{F}} \{\zeta_s \cdot (c_i^s s_i + c_i^p \Delta P_i) - c_i^e E_i^{ch}\}. \quad (1)$$

⁴The leader knows the cost function mapping of the follower in this game. The follower, on the other hand, observes the strategies from the leader and always has to take them into account.

TABLE III
NOTATION SUMMARY (ALPHABETICAL ORDER)

Variables	
b_i^k	Continuous variable, battery level (kWh) of type k vehicle when arrived at node i
ΔP_i	Continuous variable, upgrade capacity of the transformer connecting node i
q_i^k	Continuous variable, load level (kg) of type k vehicle when arrived at node i
s_i	Integer variable, number of charging ports installed in the charging station at node i
τ_i	Integer variable, time when a vehicle arrived at node i
x_{ij}^k	Binary variable, whether vehicle of type k visits node j after node i
y_i	Binary variable, whether a charging station is constructed at node i
Sets	
\mathcal{E}^N	Sets of links in the expanded network excluding the internal links within any CS, i.e. $\mathcal{E}^{PTE} \setminus (\cup \mathcal{A}_i)$
\mathcal{F}'	Set of all dummy CS nodes, i.e. $\{\mathcal{M}_i i \in \mathcal{F}\}$
\mathcal{K}	Set of vehicle type index. The vehicle types are different in three aspects: their battery sizes (B^k), their load capacities (Q^k), and their costs (c^k)
$\mathcal{M}_i(t)$	Set of dummy nodes for CS i with whose time tracker equals t , i.e. $\{j j \in \mathcal{M}_i, t(j) = t\}$
\mathcal{N}	Set of all dummy CS nodes and customer nodes, i.e. $\mathcal{C} \cup \mathcal{F}'$
\mathcal{N}_0	Set of all nodes except the sink depot, i.e. $\mathcal{N} \cup \{D_0\}$
\mathcal{N}_{n+1}	Set of all nodes except the source depot, i.e. $\mathcal{N} \cup \{D'_0\}$
$\mathcal{N}_{0,n+1}$	Set of all nodes, i.e. $\mathcal{N} \cup \{D_0, D'_0\}$
Parameters	
B^k	Battery capacity of a type k truck, in [kWh]
c_i^p	Cost of one charging port at node i , in [\$/port]
c_i^s	Cost of substation capacity upgrade at node i , in [\$/kW]
c_i^e	Service fee charged by the charging station i , in [\$/kWh]
c^k	Cost of vehicle type k , in [\$/]
c_{ij}^k	Cost of travel from node i to node j of type k , in [\$/]
d_i	Customer demand at node i
d_{ij}	Distance between node i and node j , in [km]
Δt	Time step
$\pi_{i,t}$	Electricity price at node i at time t , in [\$/kWh]
p^{rated}	Charger rated power, in [kW]
$P_{i,t}$	Substation availability at time t , at node i , in [kW]
Q^k	Freight capacity of a type k truck, in [kg]
r^k	Energy consumption rate of type k , in [kWh/km]
t_i^e, t_i^l	Earliest arrival/Latest departure time at node i
t_i^s	Required service time of node i
t_{ij}	Travel time from node i to node j
$\zeta_{s/v}$	Capital recovery factors for the charging station and the vehicles respectively

Here, E_i^{ch} represents the total electricity delivered to E-trucks at station F_i . Based on the proposed PTEN model in Section II-B, it is calculated as

$$E_i^{\text{ch}} = p^{\text{rated}} \Delta t \cdot \sum_k \sum_{(j,m) \in \mathcal{A}_i} x_{j,m}^k. \quad (2)$$

Factor ζ_s in g^L converts the life-cycle fixed cost into its annual equivalent level, which is calculated as

$$\zeta_s = \frac{r(1+r)^{Y_s}}{(1+r)^{Y_s} - 1}, \quad (3)$$

where r is the cash discount rate and Y_s is the service life of the charging station.

When building the charging stations, the CSP should ensure adequate chargers,

$$\sum_{k \in \mathcal{K}} \sum_{(j,m) \in \mathcal{A}_i(t)} x_{j,m}^k \leq s_i \quad \forall i \in \mathcal{F}, \forall t \in \mathcal{T}_i, \quad (4)$$

and sufficient transformer capacity to supply power to the visited vehicles. If at any point of time t , the total demanded power $s_i \cdot p^{\text{rated}}$ is higher than the available capacity $y_i \cdot P_{i,t}$, then the CSP would need to consider the transformer capacity upgrade cost,

$$s_i \cdot p^{\text{rated}} - y_i \cdot P_{i,t} \leq \Delta P_i \quad \forall i \in \mathcal{F}. \quad (5)$$

There are also constraints on the station size and variable domain constraints:

$$y_i s_i^{\min} \leq s_i \leq y_i s_i^{\max} \quad \forall i \in \mathcal{F}, \quad (6)$$

$$y_i \in \{0, 1\}, s_i \in \mathbf{Z}^+, \Delta P_i \in \mathbf{R}^+, \quad \forall i \in \mathcal{F}. \quad (7)$$

B. FO's Problem: Fleet Design and Operation

The FO's goal is to decide its E-truck fleet composition and routing plans so that its overall cost is minimized. The cost objective for the FO is

$$\begin{aligned} g^F(\mathbf{x}) = & \zeta_v \sum_{k \in \mathcal{K}} \sum_{j \in \mathcal{N}} c^k x_{D_0 j}^k + \sum_{k \in \mathcal{K}} \sum_{i \in \mathcal{N}_0} \sum_{j \in \mathcal{N}_{n+1}} c_{ij}^k x_{ij}^k \\ & + \sum_{i \in \mathcal{F}} \sum_{t \in \mathcal{T}_i} (\pi_{i,t} + c_i^e) \sum_k \sum_{(j,m) \in \mathcal{A}_i(t)} p^{\text{rated}} \Delta t \cdot x_{j,m}^k. \end{aligned} \quad (8)$$

The first term in g^F represents the total E-truck purchase cost, which is converted into the equivalent annual level using ζ_v . The second term yields the traveling cost of the fleet. The last term calculates the cost of charging, where the per unit charging cost involves the electricity price $\pi_{i,t}$ plus the service fee c_i^e posed by the CSP.

Vehicle routing must respect resource constraints along the network, including time windows, payload capacity, energy, etc., which are given as follows.

1) Network Flow Constraints:

$$\sum_{k \in \mathcal{K}} \sum_{j \in \mathcal{N}_{n+1}, j \neq i} x_{ij}^k = 1 \quad \forall i \in \mathcal{C}, \quad (9)$$

$$\sum_{k \in \mathcal{K}} \sum_{j \in \mathcal{N}_{n+1}, j \neq i} x_{ij}^k \leq 1 \quad \forall i \in \mathcal{F}', \quad (10)$$

$$\sum_{j \in \mathcal{N}_0, j \neq i} x_{ji}^k - \sum_{j \in \mathcal{N}_{n+1}, j \neq i} x_{ij}^k = 0 \quad \forall i \in \mathcal{N}, \forall k \in \mathcal{K}, \quad (11)$$

Constraint (9) requires each customer to be visited once and only once, while for the expanded charging station nodes, this requirement is relaxed in (10). Flow conservation of each node, except the source and sink, is expressed by (11).

2) Time Window Constraints:

$$t_i^e \leq \tau_i \leq t_i^l \quad \forall i \in \mathcal{C} \cup D_0, D'_0, \quad (12)$$

$$\tau_j - \tau_i \geq (t_{ij} + t_i^s) x_{ij}^k - (1 - x_{ij}^k) T$$

$$\times \forall i \in \mathcal{N}_0, \forall j \in \mathcal{N}_{n+1}, \forall k \in \mathcal{K}, j \neq i, \quad (13)$$

$$t(j) - \tau_i \geq (t_{ij} + t_i^s) x_{ij}^k - (1 - x_{ij}^k) T$$

$$\times \forall i \in \mathcal{N}_0, \forall j \in \mathcal{F}', \forall k \in \mathcal{K}, j \neq i, \quad (14)$$

$$t(j) - \tau_i \leq (t_{ij} + t_i^s) x_{ij}^k + (1 - x_{ij}^k) T$$

$$\times \forall i \in \mathcal{N}_0, \forall j \in \mathcal{F}', \forall k \in \mathcal{K}, j \neq i, \quad (15)$$

$$\tau_j = \sum_{k \in \mathcal{K}} \sum_i x_{ij}^k \cdot t(j) \quad \forall i \in \mathcal{N}_0, \forall j \in \mathcal{F}' \quad (16)$$

The arrival time of a vehicle at a customer point i must respect the customer's service time window $[t_i^e, t_i^l]$ (12). For the depots, the time window is set as $[0, T]$. Constraint (13) expresses the relationship between two successive customer nodes i and j at their respective visited times. When $x_{ij}^k = 1$, then E-truck k 's arrival time at customer j depends on the traveling time between i, j and the service time at i . However, when $x_{ij}^k = 0$, i.e. j is not visited after i , then this constraint is relaxed.

Constraints (14)-(16) describe the evolution of visiting times when an E-truck is driving towards a charging station node. Since each dummy node is strictly associated with one specific time slot, the corresponding relation $x_{ij}^k = 1$ is true only if the arrival time τ_j at the charging node j matches $t(j)$, as shown in (14). Again, those constraints are relaxed if $x_{ij}^k = 0$.

3) Freight Capacity Constraints:

$$q_j^k \leq q_i^k - d_i x_{ij}^k + (1 - x_{ij}^k) Q^k \quad (17)$$

$$\times \forall i \in \mathcal{N}_0, \forall k \in \mathcal{K}, \forall j \in \mathcal{N}_{n+1}, j \neq i,$$

$$0 \leq q_i^k \leq Q^k \quad \forall k \in \mathcal{K}, \forall i \in \mathcal{N}_{0,n+1}, \quad (18)$$

Following the same modeling philosophy from above, the available freight loads at each node along the route are tracked using (17). Constraint (18) ensures that the E-trucks are never overloaded.

4) Energy Consumption/Recharge Constraints:

$$b_j^k \leq b_i^k - r^k d_{ij} x_{ij}^k + (1 - x_{ij}^k) B^k$$

$$\times \forall (i, j) \in \mathcal{E}^N, \forall k \in \mathcal{K}, j \neq i \quad (19)$$

$$b_j^k \leq b_i^k + p^{\text{rated}} \cdot \Delta t \cdot x_{ij}^k + (1 - x_{ij}^k) B^k$$

$$\times \forall (i, j) \in \mathcal{A}_z, \forall z \in \mathcal{F}, \forall k \in \mathcal{K} \quad (20)$$

Given the limited range of E-trucks, it is crucial to track available battery energy while traveling, which is modeled by (19) and (20). These constraints are relaxed when $x_{ij}^k = 0$ by using the term $(1 - x_{ij}^k) B^k$. We assume a constant energy consumption rate while traversing to customers and a constant charging rate while traversing the charging links. Visiting consecutive charging nodes at one physical location represents charging for multiple time slots.

$$b_0^k = B^k \quad \forall k \in \mathcal{K}, \quad (21)$$

$$0 \leq b_i^k \leq B^k \quad \forall k \in \mathcal{K}, \forall i \in \mathcal{N}_{n+1}, \quad (22)$$

$$b_i^k + p^{\text{rated}} \cdot \Delta t \leq B^k \quad \forall k \in \mathcal{K}, \forall i \in \mathcal{F}', \quad (23)$$

We assume all E-trucks start fully charged at depot (21). The battery is never depleted nor overcharged as enforced by (22) and (23), respectively.

5) Simultaneous Charging Constraint:

$$\sum_{k \in \mathcal{K}} \sum_{(j,m) \in \mathcal{A}_i(t)} x_{j,m}^k \leq s_i \quad \forall i \in \mathcal{F}, \forall t \in \mathcal{T}_i. \quad (24)$$

The number of simultaneous charging E-trucks must respect the physical charging station size limit.

6) Additional Variable Domains:

$$x_{i,j}^k \in \{0, 1\} \quad \forall i \in \mathcal{N}_0, \forall j \in \mathcal{N}_{n+1} \quad (25)$$

$$\tau_i \in \mathbf{Z}^+, \quad q_i, b_i \in \mathbf{R}^+ \quad \forall i \in \mathcal{N}_{0,n+1}.$$

C. Joint Problem as a Stackelberg Game

Given the CSP (leader) and FO (follower) optimization models above, we now integrate them to yield the complete joint planning problem:

$$\min_{\mathbf{y}, \mathbf{s}, \Delta \mathbf{P}} g^L(\mathbf{y}, \mathbf{s}, \Delta \mathbf{P}; \mathbf{x}^*) \quad (26a)$$

$$\text{s. to: } h^L(\mathbf{y}, \mathbf{s}, \Delta \mathbf{P}) \leq 0 \quad (26b)$$

$$(\mathbf{x}^*, \boldsymbol{\tau}^*, \mathbf{b}^*, \mathbf{q}^*) = \arg \min_{\mathbf{x}, \boldsymbol{\tau}, \mathbf{b}, \mathbf{q}} g^F(\mathbf{x}) \quad (26c)$$

$$\text{s. to: } h^F(\mathbf{s}, \mathbf{x}, \boldsymbol{\tau}, \mathbf{b}, \mathbf{q}) \leq 0.$$

The constraint set $h^L(\mathbf{y}, \mathbf{s}, \Delta \mathbf{P})$ contains (4)-(7) and $h^F(\mathbf{s}, \mathbf{x}, \boldsymbol{\tau}, \mathbf{b}, \mathbf{q})$ includes (9)-(25). For the reader's convenience, we have colored the leader's optimization variables blue and the follower's optimization variables red. Black bold variables are fixed optimization variables.⁵

A key benefit of the proposed PTEN is the overall mathematical formulation (26) maintains a mixed integer linear programming structure. However, solving this model is still highly non-trivial. The main challenges are twofold: (i) The overall model is a bi-level mixed integer problem (Bi-MILP) and integer variables exist in both the upper and lower levels. In this case, the commonly-used KKT (Karush-Kuhn-Tucker)-based single-level reformulation method is not applicable. (ii) The electric vehicle routing problem, embedded as the essential part of the overall problem, is an NP-hard problem whose scale grows dramatically with the size of the network. This holds true even with the partial time expansion, which mitigates but does not eliminate the computational complexity.

IV. SOLUTION ALGORITHM DESIGN

To solve this complex problem, the framework is broken down to be solved in an iterative fashion. A diagram flow in Fig.4 offers a more straightforward visualization of the overall architecture.

⁵We would emphasize that although this is a fleet sizing, facility siting and sizing, and vehicle routing joint decisions, the model is also able to consider the current existing charging network. We simply convert the corresponding decision variables to input parameters. It is a degenerate case of our model.

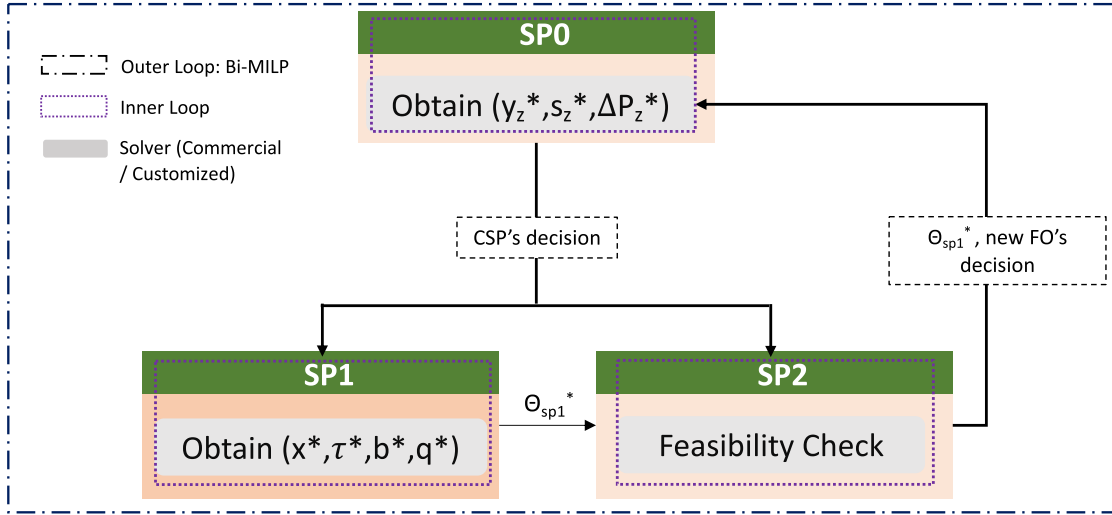


Fig. 4. The overall solution architecture. Notice that (SP2) has been detailed in Section IV-A.2. It serves as a CSP feasibility check to evaluate the solution set from its successor (SP1). Its reformulation follows the exact same process from Section IV-B.

A. Outer-Loop: Solving Bi-MILP With Reformulation and Decomposition

To address the first challenge (i), we facilitate the overall computation of the Bi-MILP with a reformulation and decomposition method [25]. We denote this as an outer loop design. The main idea of this approach and the problem-specific implementation are presented below and readers are referred to the original references for further theoretical details.

1) *Reformulation*: A key observation is that when all discrete variables in the lower-level FO problem are fixed, then the FO (26c) becomes a pure linear program with continuous decision variables. Then the optimal solution can be represented using KKT conditions. Given a specific realization for the z -indexed combination of the lower level discrete variables $\mathbf{x}^z, \boldsymbol{\tau}^z$, we denote the corresponding KKT conditions as $\Lambda(\mathbf{x}^z, \boldsymbol{\tau}^z)$. Therefore, if one enumerates all possible combinations of the follower's discrete decisions, we can denote their collection using index set $\mathcal{L}_{\text{full}} = \{1, \dots, l^{\max}\}$ where $z \in \mathcal{L}_{\text{full}}$. Then the original problem can be equivalently formulated as a single-level problem:

$$(\mathbf{P0}) \quad \min \quad g^L(\mathbf{y}, \mathbf{s}, \Delta \mathbf{P}, \mathbf{x}^0) \quad (27)$$

$$\text{s. to: } h^L(\mathbf{y}, \mathbf{s}, \Delta \mathbf{P}) \leq 0, \quad (28)$$

$$h^F(\mathbf{s}, \mathbf{x}^0, \boldsymbol{\tau}^0, \mathbf{b}^0, \mathbf{q}^0) \leq 0, \quad (29)$$

$$\forall z \in \mathcal{L}_{\text{full}}$$

$$g^F(\mathbf{x}^0) \leq g^F(\mathbf{x}^z), \quad (30)$$

$$\mathbf{y}, \mathbf{s}, \Delta \mathbf{P}, \mathbf{b}^z, \mathbf{q}^z \in \Lambda(\mathbf{x}^z, \boldsymbol{\tau}^z). \quad (31)$$

Variables $\mathbf{x}^0, \boldsymbol{\tau}^0, \mathbf{b}^0, \mathbf{q}^0$ are duplications of the follower's decisions. Constraint (30) requires that the FO's objective is at least the same, if not improved, from the discrete (and previous as we shall see) realization \mathbf{x}^z . Notably, in our case the discrete variables $\mathbf{x}, \boldsymbol{\tau}$ uniquely define the routes of the fleet. Once all routes are realized, then values of \mathbf{b}, \mathbf{q} are implicitly determined. The complexity of (31) can thus be largely reduced.

2) *Decomposition*: Instead of directly solving the complete problem (P0) with all possible combinations of $\{\mathbf{x}, \boldsymbol{\tau}, \mathbf{b}\}$ enumerated, one may solve the problem with a subset \mathcal{L}_{sub} of these combinations, i.e. $z \in \mathcal{L}_{\text{sub}} \subseteq \mathcal{L}_{\text{full}}$ and gradually enlarge the set. As explained in [25], the solution of (P0) can be obtained by iteratively solving the following decomposed parts,

- A restricted version of (P0) with the subset $\mathcal{L}_{\text{sub}} \subseteq \mathcal{L}_{\text{full}}$, denoted as (SP0). Since only a subset of all the constraints are considered during each iteration (with fixed $\mathbf{x}^z, \boldsymbol{\tau}^z$ in (30)-(31)), (SP0) provides a lower bound to the original problem (P0).
- Subproblem 1 (SP1) finds the follower's corresponding best response $\{\mathbf{x}^*, \boldsymbol{\tau}^*, \mathbf{b}^*, \mathbf{q}^*\}$ to the leader's decisions $\{\mathbf{y}^*, \mathbf{s}^*, \Delta \mathbf{P}^*\}$ from (SP0), i.e.

$$(\mathbf{SP1}) \quad \min_{\mathbf{x}, \boldsymbol{\tau}, \mathbf{b}, \mathbf{q}} \quad g^F(\mathbf{x}) \quad (32)$$

$$\text{s. to: } h^F(\mathbf{s}^*, \mathbf{x}, \boldsymbol{\tau}, \mathbf{b}, \mathbf{q}) \leq 0, \quad (33)$$

- Subproblem 2 (SP2) performs a feasibility check⁶ and is defined as

$$(\mathbf{SP2}) \quad \min_{\mathbf{x}, \boldsymbol{\tau}, \mathbf{b}, \mathbf{q}} \quad g^L(\mathbf{y}^*, \mathbf{s}^*, \Delta \mathbf{P}^*; \mathbf{x}) \quad (34)$$

$$\text{s. to: } g^F(\mathbf{x}) \leq \theta_{\text{sp1}}^*, \quad (34)$$

$$h^F(\mathbf{s}^*, \mathbf{x}, \boldsymbol{\tau}, \mathbf{b}, \mathbf{q}) \leq 0,$$

where θ_{sp1}^* is the optimal value from (SP1). When a solution is found feasible in (SP2), then the decision set $\{\tilde{\mathbf{x}}^*, \tilde{\boldsymbol{\tau}}^*, \tilde{\mathbf{b}}^*, \tilde{\mathbf{q}}^*\}$ represents the most favorable follower action for the leader. We then add it into \mathcal{L}_{sub} in (SP0) for the next round of iteration. (SP2) provides θ_{sp2}^* as an upper bound for (P0), since it clearly finds a feasible solution.

The pseudo code is detailed in Algorithm 1.

⁶Sometimes there may be multiple non-unique lower-level optimal solutions given the upper-level decision. By solving (SP2), we select the follower solution that is most in favor of the leader.

Algorithm 1 Algorithm for the Joint Planning Bi-MILP**Input:** model parameters and convergence margin ϵ **Output:** optimal solution for both CSP and FO

- Initialization:

1: Set $LB = -\infty$, $UB = \infty$, and $l = 0$

- Loop Process:

2: **while** $UB - LB > \epsilon$ **do**3: Solve (SP0) with current combinations $z = 1, \dots, l^{\text{sub}}$ and obtain $\{y_z^*, s_z^*, \Delta P_z^*\}$ and the optimal objective Θ_{RMP}^* , set $LB = \Theta_{\text{RMP}}^*$.4: Solve (SP1) given $\{y_z^*, s_z^*, \Delta P_z^*\}$ as fixed, and obtain $\{x^*, \tau^*, b^*, q^*\}$ and the optimal objective as θ_{sp1}^* 5: Solve (SP2) with $\{y_z^*, s_z^*, \Delta P_z^*\}$ as fixed, and obtain $\{\tilde{x}^*, \tilde{\tau}^*, \tilde{b}^*, \tilde{q}^*\}$ and the optimal objective as θ_{sp2}^* 6: **if** (SP2) is feasible **then**7: Set $\{x^{z+1}, \tau^{z+1}\}$ as $\{\tilde{x}^*, \tilde{\tau}^*\}$,
 $UB = \min\{UB, \theta_{\text{sp2}}^*\}$ 8: **else**9: Set $\{x^{z+1}, \tau^{z+1}\}$ as $\{x^*, \tau^*\}$ 10: **end if**11: Add the new optimal cut corresponding to $\{x^{z+1}, \tau^{z+1}\}$ to the (SP0), set $z = z + 1$.12: **end while**13: **return** $y_z^*, s_z^*, \Delta P_z^*, x^z, \tau^z, b^z$ **B. Inner Loop: Solving E-V/LRP**

Notice that the three subproblems are structurally similar and the electric vehicle routing problem serves as the core in (SP1) and (SP2) and the location planning is encoded in (SP0). Since novel computation algorithms are not the focus of this work, for the analysis in Section V we rely on a commercial solver (e.g. Gurobi) to solve these subproblems. However, one can reformulate these problems as generalized set-partitioning problems and subsequently solve them in an iterative fashion to reduce computational burden when the network size becomes very large, possibly sacrificing solution quality. We refer interested readers to [11] for set-partitioning reformulation.

V. CASE STUDIES

We have proposed an optimization modeling framework and iterative algorithm to solve this problem. To effectively demonstrate the model, we deliberately design a small but intuitive network. We will highlight some of the binding features, like the customer time windows and the charging rates.

The small network is presented in Fig. 5. It consists of 1 depot node D_0 , 5 customer nodes $\mathcal{C} = \{A, B, C, D, E\}$ and 2 candidate charging station nodes $\mathcal{F} = \{F_1, F_2\}$. The dashed lines are the feasible links with adjacent numbers indicating the lengths. We summarize all relevant parameters for CSP in Table IV⁷ and for the FO in Table V. Next, we will numerically demonstrate the necessity of the two-entity modeling. Then,

⁷We keep the station available capacity $P_{i,t}$ constant over time for convenience. It's not the main focus of this study.

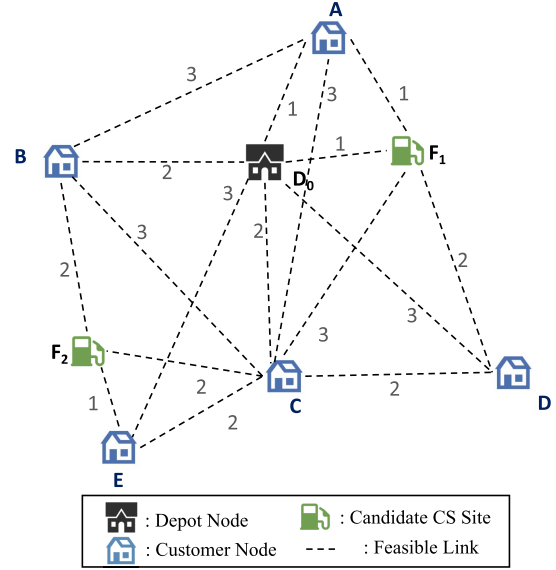


Fig. 5. Small network (original).

we will study the cost breakdowns and the varying dynamics when stricter time windows are applied and charging rates are varied.

A. Base Case: Necessity of Considering Different Entities

We first focus on the different strategies when a social planner (single entity) or non co-operation (two entities) is considered. Simulations are performed for both scenarios with the service fee varying from 0 to 0.5(\$/kWh).⁸ The results obtained are given in Fig.6.

Consider the single entity scenario. To enable a fair comparison against the two-entity case, we plot the combined costs of electricity and service fee ($\pi_i + c_i^e$) for the single entity. Together they will jointly affect the vehicle routing, charging, as well as the infrastructure decisions. When the service fee is set to 0, the FO charges at the cost of electricity (π_i) purchased from the utility, i.e. with zero profit margin. Given the optimized planning results, we then split and plot the corresponding costs to the FO and CSP. In greater detail, the FO cost consists of the fleet investment, travel expenditure as well as the combined cost of electricity and service fee; on the other hand, the CSP cost is the infrastructure investment less the profits from providing service. The cost splits are presented by the dashed lines in Fig. 6 and the colored shape labels on the dashed line indicate the different optimal strategies corresponding (see Table VI) to each simulated price value. Note that when service fee is set at \$0/kWh, this is the case commonly known as to minimize the total cost of ownership (TCO) in literature. However, as shown in the left most in Fig.6, it actually induces the largest cost to the CSP.

For the two-entities scenario, we solve the problem with the proposed model. We superimpose the costs for the FO and CSP in Fig. 6 using solid lines. It is visually clear that the decisions under the two-entity scenario achieves lower net costs than the single entity scenario most of the time,

⁸We leave customer time windows sufficiently wide in this case.

TABLE IV
PARAMETERS OF CANDIDATE CHARGING STATIONS

Station ID	Available capacity (kW)	Charge rate (kW)	Cost of charger (\$)	Substation upgrade cost (\$/kW)	Electricity cost (\$/kWh)
F_1	15	5	10000	788	0.1
F_2	30	10	10500	788	0.1

TABLE V
VEHICLE PARAMETERS

Vehicle ID	Freight capacity (kg)	Battery capacity (kWh)	Energy consumption (kW/unit length)	Vehicle cost (\$)	Travel cost (\$/unit length)
1	150	50	10	10000	0.5
2	200	60	10	18000	0.5

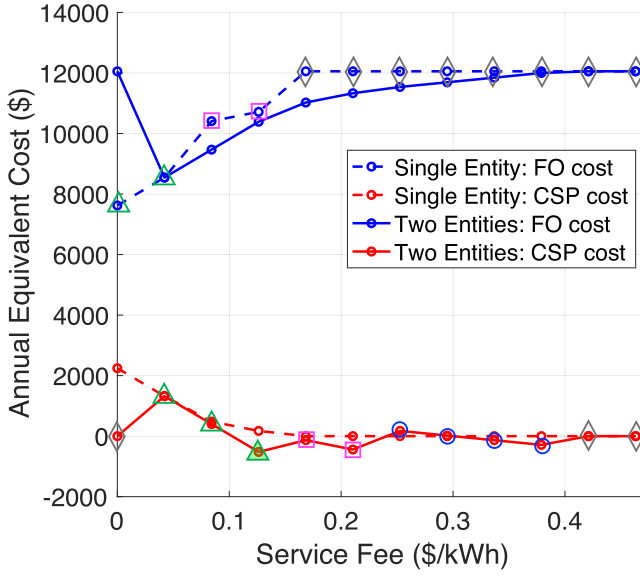


Fig. 6. Cost of different players with respect to different service fee, without time windows. The colored marker shapes correspond to different strategies in Table VI. The markers on the upper dashed blue line correspond to the single entity case, whereas the markers on the lower solid red line correspond to the two-entity case.

i.e. the FO achieves lower costs and the CSP generates more profit. The only exceptions happen when the service fees are extremely low (below \$0.05/kWh). Within this range, from a pure economic point of view, the CSP has little to no interest to invest and enter the market.⁹ The CSP can be incentivized to participate by increasing the service fee. However, as the CSP becomes more “greedy,” the FO will reject the option to charge at the facility. This then leads to a non-cooperative situation, as indicated by the grey rhombuses on the solid line in Fig. 6 (after service fee is more than \$0.421/kWh).

Since the CSP is the leader in the game, it will naturally take advantage of being the first-mover. The final decision for the CSP is to build charging stations at both locations with service fee set at 0.125 \$/kWh in this particular example (solid green triangle in Fig. 6). The corresponding fleet routes are shown in Fig. 7 (Plan 2). We denote the first/second route chosen by E-truck-1/2 as route 0/1 for later reference. Indeed, it is the most efficient and straightforward to assume the

⁹Even if the CSP enters (the second green triangle), it is not at all cost-attractive. It experiences positive cost and no profit.

TABLE VI
POSSIBLE STRATEGY-PAIRS IN BASE CASE

Plan	FCS	Routing Plan
1(\diamond)	None	E-truck-1 of type 1: $D_0 \rightarrow B \rightarrow D_0$ E-truck-2 of type 2: $D_0 \rightarrow A \rightarrow C \rightarrow D_0$ E-truck-3 of type 2: $D_0 \rightarrow E \rightarrow D_0$ E-truck-4 of type 2: $D_0 \rightarrow D \rightarrow D_0$
2(\triangle)	F_1, F_2	E-truck-1 of type 1: $D_0 \rightarrow D \rightarrow F_1 \rightarrow A \rightarrow D_0$ E-truck-2 of type 1: $D_0 \rightarrow B \rightarrow F_2 \rightarrow E \rightarrow C \rightarrow D_0$
3(\square)	F_1	E-truck-1 of type 1: $D_0 \rightarrow B \rightarrow D_0$ E-truck-2 of type 2: $D_0 \rightarrow A \rightarrow F_1 \rightarrow D \rightarrow C \rightarrow D_0$ E-truck-3 of type 2: $D_0 \rightarrow E \rightarrow D_0$
4(\circ)	F_1	E-truck-1 of type 2: $D_0 \rightarrow B \rightarrow A \rightarrow D_0$ E-truck-2 of type 2: $D_0 \rightarrow F_1 \rightarrow D \rightarrow C \rightarrow D_0$ E-truck-3 of type 2: $D_0 \rightarrow E \rightarrow D_0$

existence of a powerful social planner. However, this common assumption in the literature is not always the case in real life. We further emphasize an important nuance here: only through rigorous and comprehensive cost analysis can we incentivize both entities to come up with an agreement that benefits both sides, even though the eventual outcome does not always lead to the social optimum as contests prevail.¹⁰

B. The Effects of Customer Time Windows and Charging Rates

We are going to show how two of the binding features, time windows and charging rates, will influence optimal decisions. We set tighter delivery time windows for customer B, C and D as [1, 4], [6, 9], [2, 3] respectively. First, we keep the charge rate as 10 kW as in the base case and the results are plotted in Fig. 8. In this case, the FO will reject charging service from the CSP when the price exceed 0.25 \$/kWh. This critical threshold was 0.421 \$/kWh in the base case (Section V-A), where no time windows are set. The only profitable service fee for the CSP occurs 0.1684 \$/kWh, whereas all other services fees yield zero or negative profit. Note, in the base case, there were

¹⁰Note that this is an one-to-one service scenario. More involved settings and further analysis can be extended to one-to-many or many-to-one scenarios. This is out of scope and we will leave it for future work.

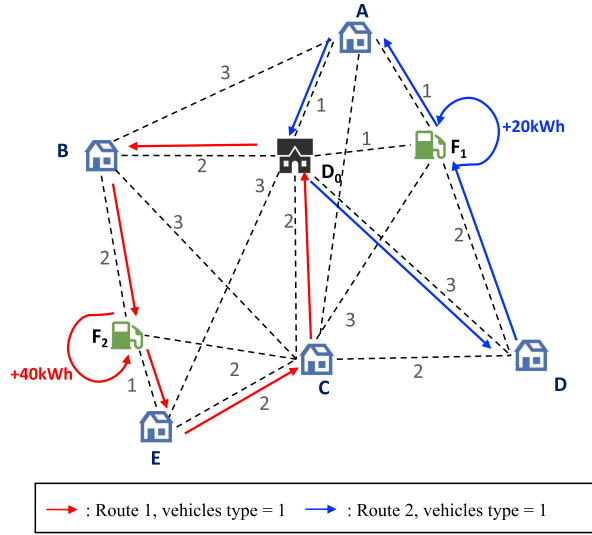


Fig. 7. Optimal routes of FO.

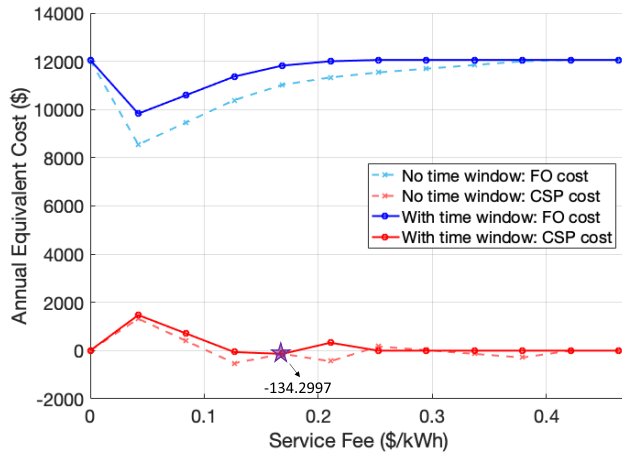


Fig. 8. With time windows, cost of different players with respect to different service fee. The two upper curves correspond to the FO costs; the lower two are the CSPs'.

TABLE VII

SELECTED STRATEGY WHEN TIGHTER TIME WINDOWS ARE APPLIED

Plan	FCS	Routing Plan
1(★)	F_1	E-truck-1 of type 1: $D_0 \rightarrow B \rightarrow D_0$
		E-truck-2 of type 1: $D_0 \rightarrow C \rightarrow D_0$
		E-truck-3 of type 1: $D_0 \rightarrow E \rightarrow D_0$
		E-truck-4 of type 2:
		$D_0 \rightarrow D \rightarrow F_1 \rightarrow A \rightarrow D_0$

six profitable service fees. However, the profit now is 74.23% lower than that in the base case.

In this example, some tightened time windows significantly reduced the number of feasible routes for the FO. It becomes a tougher decision to balance both time spent for charging and time to meet customers. The previously selected route 1 ($D_0 \rightarrow B \rightarrow F_2 \rightarrow E \rightarrow C \rightarrow D_0$) becomes infeasible as the E-trucks need 4 units of time to charge (to complete the trip) but will miss customer C. As a result, three separate E-trucks are purchased instead to serve customer B, C and E respectively. The detailed plan is given in Table VII. This increases the final cost of the FO by 13.8%.

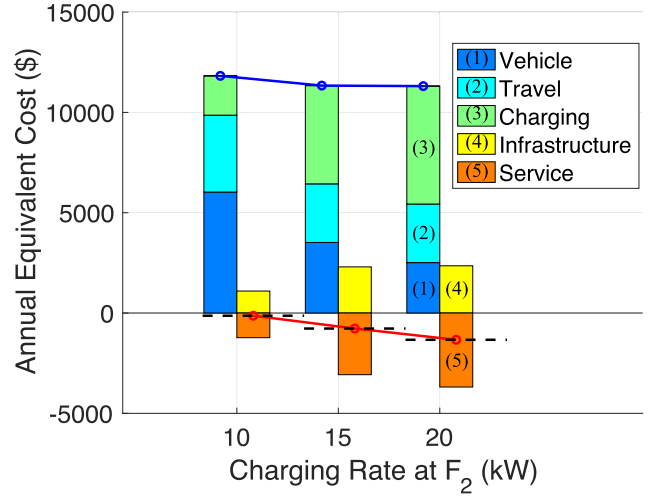
Fig. 9. Costs of different players with different charging rate at F_2 . Upper solid line is the net annual equivalent costs of the FO and the lower dashed line is the net profits of the CSP.

TABLE VIII

PLAYERS' STRATEGIES WITH DIFFERENT CHARGING RATES

Rate	CSP's Strategy	FO's Strategy
10kW	F_1	Number of E-truck of type 1: 2 Number of E-truck of type 2: 2 Enroute charging: 20kWh
15kW	F_1, F_2	Number of E-truck of type 1: 1 Number of E-truck of type 2: 1 Enroute charging: 50kWh
20kW	F_1, F_2	Number of E-truck of type 1: 2 Number of E-truck of type 2: 0 Enroute charging: 60kWh

One alternative solution that may realize benefits to both sides is to increase the chargers' charging rate. The cost breakdowns over the variations of rate are shown in Fig. 9. They are plotted with respect to the two entities – the FO on the left and the CSP on the right. Black dashed lines indicate the CSP's overall net cost/profit (for positive/negative values resp.). The corresponding strategies are also listed in Table VIII. We see that when the rate increases from 10 kW to 15 kW, the previously selected route 1 can again be assigned to a larger E-truck, whereas when the rate is doubled, the smaller E-truck may be used. Although more charging energy is needed, the trucks still meet all the delivery time windows. As a result, reductions in E-truck fleet investment and travel cost compensate the extra charging expenditure and lead to overall FO cost savings. From the CSP's perspective, although more infrastructure investment is required¹¹ up-front, it also realizes more profit gains. The increased revenues from energy service cover the increased capital costs.

¹¹The cost for a single port is assumed to increase with the charging rate. Indeed the infrastructure investments at 15 and 20 kW are subtly different.

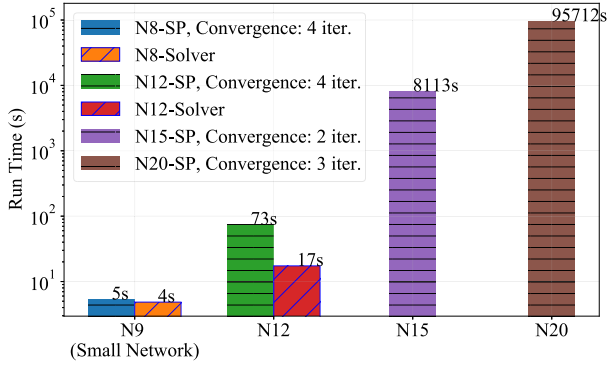


Fig. 10. Computation Time for 4 Different Instances. Since the commercial solver (denoted “-Solver”) is not able to handle the latter two instances (freezes over 100,000s), we have reformulated the problem as a set-partitioning (SP) problem and solved.

We have illustrated two of the binding features along with the dynamic interactions between the two entities. This is indeed a complex but more realistic situation, as opposed to existing work that considers a single entity only. We have demonstrated that without assuming the existence of a powerful social planner, careful analysis is needed to contemplate and incentivize both parties to collaborate. With our framework, the FOs and the CSPs can now look for their operation “sweet spots” and be more committed to transportation electrification.

C. Complex Network Study

For this work, we highlight the modeling contribution, rather than any algorithmic superiority. However, to analyze the computational burden and results as network size grows, we synthetically generated three larger instances. There are 12, 15, 20 nodes in the instances respectively. Each instance has three candidate charging station nodes. The total number of nodes and edges are calculated after partial time expansion at the three candidate sites. These are fully connected graphs and the networks after expansion contain thousands of edges (summarized in Table IX). Since the commercial solver is not able to handle the latter two instances, we reformulated the subproblems as a set-partitioning problem and solve iteratively. The computational times are summarized in Fig. 10

The parameters used in these instances are summarized in Table X and Table XI. These parameters are adopted to reflect practice: customers are more spatially distributed, the E-truck ranges and energy consumption are taken from vehicle specifications announced by the manufacturers, and all cost parameters are adopted from [21], [30], [31], [32], and [33]. We demonstrate that the outer-loop algorithm from Section IV-A empirically converged in much fewer iterations as compared to the enormous set $\mathcal{L}_{\text{full}}$ (Table IX). Our results align with the findings in [17]. In fact, these iterations may be interpreted as a negotiation process between the leader (CSP) and the follower (FO). While solving the leader problem in (SP0), (30) upper bounds the follower’s objective and ensures it decreases (or stays the same) at each iteration. With this (follower’s response) in mind, the leader proposes a design and operational plan until an optimal proposal is accepted by both entities.

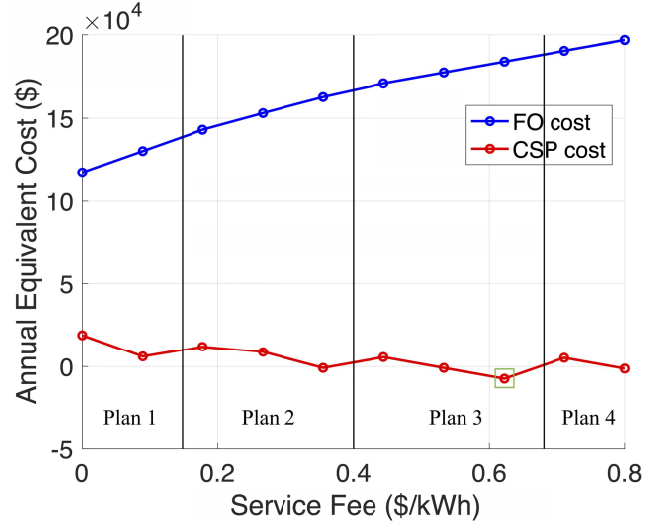


Fig. 11. Cost of different players with respect to different service fees. The green rectangle in the figure indicates the best action of CSP, which yields the most profits.

The non-cooperative nature of the two entities holds for these larger instances. We will share N12 as an example in Fig. 11. There are four possible strategy pairs for the leader (CSP) and follower (FO) detailed in Table XII, corresponding to different service fees imposed by the CSP. With smaller service fees, such as Plan 1, the CSP is not willing to open more than one charging station to provide service; on the other hand, when the service fee is high, such as Plan 4, the CSP will invest heavily and open all stations. In Plan 4, however, the CSP faces the risk that the FO deploys more E-trucks to accommodate customer demand yet reduce charging needs, which increases the FO’s cost but decreases the CSP’s revenue. As Fig. 11 demonstrates, the best strategy for the CSP is actually Plan 3, where the CSP finds the most profitable action is to open 2 charging stations and the FO deploys 5 E-trucks to fulfill customer demand.

D. One-to-Multiple Generalization

This work studies in depth the non-cooperative nature between the charging service provider (CSP) and the truck fleet operator (FO), a one-to-one interactive setting. However, this framework can also be generalized to a one-to-multiple setting, where multiple fleet operators charge through a single service provider. In reality, logistic companies provide delivery services through bilateral contracts with individual customers. This is unlike an open market, where different suppliers compete for customers with bid offers. In fact, about 80% of this market is based on long-term contractual agreements. Each truck fleet operator has pre-determined the specific portfolio of customer locations and demands. Hence, to model multiple FOs in the problem, we consolidate these fleet operators and simply introduce the idea of a “Super FO”. Relevant constraints like (4) (the charger constraint) can be extended to the following,

$$\sum_{\phi \in \Phi} \sum_{k \in \mathcal{K}_{\phi}} \sum_{(j,m) \in \mathcal{A}_i(t)} x_{j,m}^{k\phi} \leq s_i \quad \forall i \in \mathcal{F}, \forall t \in \mathcal{T}_i, \quad (35)$$

TABLE IX
CONFIGURATIONS OF INSTANCES

Instance Name	Number of Nodes	Number of Candidate Charging Station Nodes	Number of Nodes (Expanded)	Number of Edges	Iterations to Converge
N12	12	3	201	3,712	4
N15	15	3	204	4,924	2
N20	20	3	209	6,984	3

TABLE X
VEHICLE PARAMETERS

Vehicle Type [32]	Freight Capacity (kg)	Battery Capacity (kWh) [32]	Energy Consumption (kWh/km) [33]	Cost of Vehicle (\$) [21]
1	250	350	1.44	100000
2	180	260	1.44	66000

TABLE XI
MISCELLANEOUS PARAMETERS

Name (unit) [Source]	Value
Capital Recovery Factor [30]	0.10
Charge Rate (kW)	200
Cost of Charger (\$/port) [21]	185000
Cost of capacity upgrade (\$/kW) [21]	788
Discount factor [30]	0.06
Life year [21]	15
Road length range (km)	[70, 140]
Speed (km/h) [31]	88
Time horizon (hour)	12
Time steps	24

TABLE XII
POSSIBLE STRATEGY-PAIRS FOR N12

Plan	CSP Decisions	FO Decisions
1	open 1 station	4 Type 1 E-truck
2	open 2 stations	4 Type 1 E-truck
3 (□)	open 2 stations	5 Type 1 E-truck
4	open 3 stations	6 Type 1 E-truck

where notation Φ represent the set of fleet operators. On the other hand, we would like to point out that if competition prevails among the fleet operators to use the chargers (i.e. charging demand exceeds supply), then the notion of “Super FO” may not exist. A study of market equilibrium becomes necessary. However, this is out of the scope of this work.

VI. CONCLUSION

This work proposes a new modeling framework to capture the non-cooperative interactions between a charging service provider (CSP) and fleet operator (FO) in the joint charging network design and mobility planning problem. This reflects reality, in which the two entities are separate self-optimizing organizations. To consider the charging station capacity, this work also proposes, for the first time, a partial time expanded network. It enables jointly optimizing the size of the charging infrastructure in the classic location routing problem regime. The non-cooperative interaction is formulated in a Stackelberg game framework as a Bi-MILP problem. The solution framework was broken down to be solved in an iterative fashion.

We find that non-cooperation between these two entities can lead to lower total costs than a single entity scenario. Detailed numerical studies demonstrate the effects of binding features and provide insights to interested players. The nature of the solutions with a single social planner and two non-cooperative

entities can be dramatically different. Our framework examines these distinct aspects and hence provide more reliable results to the case in real life. In the end, we have also included a discussion about the generalization from one to multiple FOs setting.

ACKNOWLEDGMENT

The authors would like to thank Dr. Anna Robert for providing constructive feedbacks.

REFERENCES

- [1] USEPA. (2020). *Fast Facts: U.S. Transportation Sector Greenhouse Gas Emissions 1990–2018*. [Online]. Available: <https://nepis.epa.gov/Exe/ZyPDF.cgi?Dockey=P100ZK4P.pdf>
- [2] J. Gerdes. (2020). *Next Up for Electrification: Heavy-Duty Trucks and Construction Machinery*. [Online]. Available: <https://www.greentechmedia.com/articles/read/next-up-for-electrification-heavy-duty-trucks-and-construction-machinery>
- [3] J. Yang and H. Sun, “Battery swap station location-routing problem with capacitated electric vehicles,” *Comput. Oper. Res.*, vol. 55, pp. 217–232, Mar. 2015.
- [4] J. Hof, M. Schneider, and D. Goeke, “Solving the battery swap station location-routing problem with capacitated electric vehicles using an AVNS algorithm for vehicle-routing problems with intermediate stops,” *Transp. Res. B, Methodol.*, vol. 97, pp. 102–112, May 2017.
- [5] M. Schiffer, S. Stütz, and G. Walther, “Are ecvs breaking even?—Competitiveness of electric commercial vehicles in medium-duty logistics networks,” RWTH Aachen Univ., Aachen, Germany, Tech. Rep. OM-02/2016, 2016.
- [6] M. Schiffer, M. Schneider, and G. Laporte, “Designing sustainable mid-haul logistics networks with intra-route multi-resource facilities,” *Eur. J. Oper. Res.*, vol. 265, no. 2, pp. 517–532, Mar. 2018.
- [7] M. Schiffer and G. Walther, “An adaptive large neighborhood search for the location-routing problem with intra-route facilities,” *Transp. Sci.*, vol. 52, no. 2, pp. 331–352, 2017.
- [8] M. Schiffer and G. Walther, “Strategic planning of electric logistics fleet networks: A robust location-routing approach,” *Omega*, vol. 80, pp. 31–42, Oct. 2018.
- [9] M. Schiffer and G. Walther, “The electric location routing problem with time Windows and partial recharging,” *Eur. J. Oper. Res.*, vol. 260, no. 3, pp. 995–1013, 2017.
- [10] W. Li-ying and S. Yuan-bin, “Multiple charging station location-routing problem with time window of electric vehicle,” *J. Eng. Sci. Technol. Rev.*, vol. 8, no. 5, pp. 1–12, 2015.
- [11] G. Hiermann, J. Puchinger, S. Ropke, and R. F. Hartl, “The electric fleet size and mix vehicle routing problem with time Windows and recharging stations,” *Eur. J. Oper. Res.*, vol. 252, no. 3, pp. 995–1018, Aug. 2016.
- [12] C. Prodhon and C. Prins, “A survey of recent research on location-routing problems,” *Eur. J. Oper. Res.*, vol. 238, no. 1, pp. 1–17, 2014.
- [13] M. Schiffer, M. Schneider, G. Walther, and G. Laporte, “Vehicle routing and location routing with intermediate stops: A review,” *Transp. Sci.*, vol. 53, no. 2, pp. 319–343, 2019.
- [14] X. Zhang et al., “Bilevel optimization based transmission expansion planning considering phase shifting transformer,” in *Proc. North Amer. Power Symp. (NAPS)*, 2017, pp. 1–6.

- [15] M. Asensio, G. Muñoz-Delgado, and J. Contreras, “Bi-level approach to distribution network and renewable energy expansion planning considering demand response,” *IEEE Trans. Power Syst.*, vol. 32, no. 6, pp. 4298–4309, Nov. 2017.
- [16] S. Tabrizi, S. H. Ghodspour, and A. Ahmadi, “Modelling three-echelon warm-water fish supply chain: A bi-level optimization approach under Nash–Cournot equilibrium,” *Appl. Soft Comput.*, vol. 71, pp. 1035–1053, Oct. 2018.
- [17] D. Yue and F. You, “Stackelberg-game-based modeling and optimization for supply chain design and operations: A mixed integer bilevel programming framework,” *Comput. Chem. Eng.*, vol. 102, pp. 81–95, Jul. 2017.
- [18] E. Zavvos, E. H. Gerding, and M. Brede, “A comprehensive game-theoretic model for electric vehicle charging station competition,” *IEEE Trans. Intell. Transp. Syst.*, vol. 23, no. 8, pp. 12239–12250, Aug. 2021.
- [19] M. Mahmoudi and X. Zhou, “Finding optimal solutions for vehicle routing problem with pickup and delivery services with time Windows: A dynamic programming approach based on state–space–time network representations,” *Transp. Res. B, Methodol.*, vol. 89, pp. 19–42, Jul. 2016.
- [20] G. Lu, X. Zhou, Q. Peng, B. He, M. Mahmoudi, and J. Zhao, “Solving resource recharging station location-routing problem through a resource-space-time network representation,” 2016, *arXiv:1602.06889*.
- [21] H. Zhang, C. J. R. Sheppard, T. E. Lipman, and S. J. Moura, “Joint fleet sizing and charging system planning for autonomous electric vehicles,” *IEEE Trans. Intell. Transp. Syst.*, vol. 21, no. 11, pp. 4725–4738, Nov. 2019.
- [22] S. R. Kancharla and G. Ramadurai, “Electric vehicle routing problem with non-linear charging and load-dependent discharging,” *Exp. Syst. Appl.*, vol. 160, Dec. 2020, Art. no. 113714.
- [23] M. Bruglieri, S. Mancini, and O. Pisacane, “The green vehicle routing problem with capacitated alternative fuel stations,” *Comput. Oper. Res.*, vol. 112, Dec. 2019, Art. no. 104759.
- [24] S. Erdoğan and E. Miller-Hooks, “A green vehicle routing problem,” *Transp. Res. E, Transp. Rev.*, vol. 48, no. 1, pp. 100–114, Jan. 2012.
- [25] B. Zeng and Y. An, “Solving bilevel mixed integer program by reformulations and decomposition,” *Optim. online*, pp. 1–34, Jun. 2014. [Online]. Available: http://www.optimization-online.org/DB_FILE/2014/07/4455.pdf
- [26] S. Sripad and V. Viswanathan, “Quantifying the economic case for electric semi-trucks,” *ACS Energy Lett.*, vol. 4, no. 1, pp. 149–155, Jan. 2019, doi: [10.1021/acsenenergylett.8b02146](https://doi.org/10.1021/acsenenergylett.8b02146).
- [27] H. Liimatainen, O. Van Vliet, and D. Aplyn, “The potential of electric trucks—An international commodity-level analysis,” *Appl. Energy*, vol. 236, pp. 804–814, Feb. 2019. [Online]. Available: <http://www.sciencedirect.com/science/article/pii/S0306261918318361>
- [28] C. Buysse and B. Sharpe, “California’s advanced clean trucks regulation: Sales requirements for zero-emission heavy-duty trucks,” Int. Council Clean Transp., San Francisco, CA, USA, Tech. Rep., Jul. 2020. [Online]. Available: <https://theicct.org/sites/default/files/publications/CA-HDV-EV-policy-update-jul2020.pdf>
- [29] J. B. Cruz, Jr., “Survey of Nash and Stackelberg equilibrium strategies in dynamic games,” *Ann. Econ. Social Meas.*, vol. 4, no. 2, pp. 339–344, 1975.
- [30] T. Zeng, H. Zhang, and S. Moura, “Solving overstay and stochasticity in PEV charging station planning with real data,” *IEEE Trans. Ind. Informat.*, vol. 16, no. 5, pp. 3504–3514, May 2019.
- [31] C. State of California, *Truck Lane Use*. Accessed: Jun. 18, 2022. [Online]. Available: <https://dot.ca.gov/programs/traffic-operations/legal-truck-access/truck-lane-use>
- [32] S. Downing, (Jan. 2020). *8 Electric Truck and Van Companies to Watch in 2020*. [Online]. Available: <https://www.greenbiz.com/article/8-electric-truck-and-van-companies-watch-2020>
- [33] T. Earl, L. Mathieu, S. Cornelis, S. Kenny, C. C. Ambel, and J. Nix, “Analysis of long haul battery electric trucks in EU,” in *Proc. 8th Commercial Vehicle Workshop*, 2018, pp. 1–22.



Yiqi Zhao was born in Handan, Hebei, China, in January 1995. She received the Bachelor of Science (B.Sc.) degree in field of electrical engineering and its automation from Southeast University, China, in 2014, the Master of Science (M.Sc.) degree in field of electrical engineering from the KTH Royal Institute of Technology in 2016, and the Doctor of Philosophy (Ph.D.) degree from the Department of Electrical Engineering, Tsinghua University, in 2021. Her research interests lie in the area of electric vehicle, charging facility planning, and smart grid.



Teng Zeng received the B.S. degree in energy engineering and the M.S. degree in systems engineering from the University of California at Berkeley, Berkeley, in 2018 and 2019, respectively. He is currently pursuing the Ph.D. degree in systems engineering with the Civil and Environmental Engineering Department.

His research interests include optimization and control in the area of plug-in electric vehicles and infrastructure planning and operation.



Zaid Allybokus was born in Mauritius in June 1989. He received the joint M.Sc. degree in the field of optimization, games and control from the Ecole Normale Supérieure de Paris and the Université Pierre et Marie Curie, Paris, in 2015, and the joint Ph.D. degree in applied mathematics from the University of Nice Côte d’Azur, based at Huawei Technologies, Boulogne-Billancourt, and INRIA Sophia Antipolis, where he focused on routing and real-time resource allocation problems in distributed software-defined networks. Since 2019, he has been a Research Engineer specialized in optimization at TotalEnergies OneTech. His current research activities include e-mobility, real-time control of green energy assets, and infrastructure planning and management. He won the best paper award at the International Teletraffic Congress in 2017.



Ye Guo (Senior Member, IEEE) received the bachelor’s and Ph.D. degrees from the Department of Electrical Engineering, Tsinghua University, in 2008 and 2013, respectively. He is currently an Associate Professor at the Tsinghua-Shenzhen International Graduate School, Tsinghua University. He was a Post-Doctoral Associate at Cornell University between 2014 and 2018. His research interests include distributed optimization, game and market theory, state estimation, and their applications in power and energy systems. From 2019 to 2021, he won IEEE PES General Meeting best paper awards four times for three years in a row, one coauthored paper selected as the “Best-of-the-Best Paper Award.”



Scott Moura (Member, IEEE) received the B.S. degree from the University of California at Berkeley, Berkeley, CA, USA, in 2006, and the M.S. and Ph.D. degrees from the University of Michigan, Ann Arbor, in 2008 and 2011, respectively, all in mechanical engineering. He is currently an Associate Professor in civil and environmental engineering and the Director of the Energy, Controls, & Applications Laboratory (eCAL), University of California at Berkeley. He is also a Faculty Member of the Tsinghua-Berkeley Shenzhen Institute.

From 2011 to 2013, he was a Post-Doctoral Fellow of the Cymer Center for Control Systems and Dynamics, University of California at San Diego, San Diego. In 2013, he was a Visiting Researcher at the Centre Automatique et Systèmes, MINES ParisTech, Paris, France. His research interests include control, optimization, machine learning for batteries, electrified vehicles, and distributed energy resources.

He was a recipient of the National Science Foundation (NSF) Career Award, Carol D. Soc Distinguished Graduate Student Mentor Award, the Hellman Fellowship, the O. Hugo Shuck Best Paper Award, the ACC Best Student Paper Award (as an Advisor), the ACC and ASME Dynamic Systems and Control Conference Best Student Paper Finalist (as a Student and an Advisor), the UC Presidential Postdoctoral Fellowship, the NSF Graduate Research Fellowship, the University of Michigan Distinguished ProQuest Dissertation Honorable Mention, the University of Michigan Rackham Merit Fellowship, and the College of Engineering Distinguished Leadership Award.